A Molecular Dynamics Study of Aqueous Solutions
III. A Comparison of Selected Alkali Halides

K. Heinzinger and P. C. Vogel *

Max-Planck-Institut für Chemie (Otto-Hahn-Institut), Mainz, Germany

(Z. Naturforsch. **31 a**, 463–475 [1976]; received January 30, 1976)

Results of a molecular dynamics study of aqueous solutions of LiJ, LiCl, NaCl, CsCl and CsF are reported. The basic periodic box contained 200 water molecules, 8 cations and 8 anions, equivalent to 2.2 molal solutions. Static properties of the first hydration shells of the ions are discussed in detail on the basis of radial pair correlation functions, average potential energies of the water molecules and pair interaction energy distributions. The calculations lead to the conclusion that in the first hydration shells a lone pair orbital of the water molecule is directed towards the cation while a hydrogen atom points towards the anion. In the five alkali halide solutions investigated ion pairing occurs only with CsF. The hydration numbers, when defined as the volume integrals of the ion-water radial pair correlation functions up to the first minimum, increase with increasing ion size and depend on the size of the counterion. The water-water interactions in the solutions show not only features of pure water at elevated temperatures but also of pure water under compresion. The agreement between calculated and measured self diffusion coefficients is still insufficient.

I. Introduction

In two previous papers from this laboratory [1, 2] preliminary results of molecular dynamics calculations on 2.2 molal aqueous LiCl and CsCl solutions have been reported. Inspite of some shortcomings, especially as far as dynamical properties are concerned, the results of these investigations seemed to be promising with respect to a better understanding of the structure of aqueous solutions and justified a continuation and extension of the calculations on this line. Some other approaches to simulate aqueous salt solutions have meanwhile been studied by Gosling and Singer [3] and Rahman [4].

Our preliminary results of the calculations gave no indication not to adhere to the ST2 water model of Stillinger and Rahman [5]. In order to improve the simulation, the switching function in the ion-ion pair potential has been removed and its range has been extended up to a distance of $2^1/_2$ times the length of the basic periodic box. Some additional properties have been calculated such as the average value of the cosine between the dipole moments of the water molecules as a function of distance and the average value of the square of the total dipole moment of the water molecules within the basic box. Also the average pair potential energy of the water molecules has been plotted as a function of oxygen-oxygen distance.

Reprint requests to Dr. K. Heinzinger, Max-Planck-Institut für Chemie, Saarstr. 23, P.O.B. 3060, *D-6500 Mainz*.

* Present address: BASF Wyandotte Corp., Wyandotte, Michigan, USA.

The calculations have been extended to solutions of LiJ, NaCl and CsF. These solutions were selected in order to get information on changes of the hydration shell of an ion by a change of the counterion. This provides an other check of possible limitations of the ST2 water model as far as static properties of the aqueous solutions are concerned.

In a subsequent paper [6] the molecular dynamics results of a 0.55 molal NaCl solution are compared with the 2.2 molal solution reported here.

II. Effective Pair Potentials and Details of the Calculations

As in the previous work [1, 2] the total potential was obtained as the sum of effective pair potentials. For the water molecule the ST2 four point charge model [5] was used, while the ions were treated as point charges residing at the center of Lennard-Jones spheres.

The effective pair potentials used consist of a Lennard-Jones term (centered at the oxygen atom for the water molecules)

$$V_{ij}^{LJ}(r) = 4\,\varepsilon_{ij}\,[(\sigma_{ij}/r)^{12} - (\sigma_{ij}/r)^{6}]\,,$$

where i and j refer either to ions or water molecules, and a Coulomb term, different for water-water, ion-water and ion-ion interaction, as given by:

$$V_{\mathrm{ww}}^{\mathrm{C}}(r, d_{11}, d_{12}\ldots) = S_{\mathrm{ww}}(r)\,q^2 \sum_{\alpha,\beta=1}^{4} (-1)^{\alpha+\beta}/d_{\alpha\beta}\,,$$

$$V_{\substack{+\mathrm{w}\\(-\mathrm{w})}}^{\mathrm{C}}(d_{\substack{+1\\(-1)}}, d_{\substack{+2\\(-2)}}\ldots) = -\sum_{(+)\,\alpha=1}^{4} (-1)^{\alpha}\,q\,e/d_{\substack{+\alpha\\(-\alpha)}}\,,$$

$$V_{\substack{\pm\pm\\(+-)}}^{\mathrm{C}}(r) = \underset{(-)}{+}e^2/r\,.$$

The switching function, $S_{ww}(r)$, has been introduced by Rahman and Stillinger [7] to reduce unrealistic Coulomb forces between very close water molecules. It is given explicitly in Reference 2. $q = 0.23$ e is the charge in the ST2 model. d and r denote distances between point charges and Lennard-Jones centers. The sign of the Coulomb terms is correct if α and β are chosen to be odd for positive and even for negative charges. The Lennard-Jones parameters for the various interactions are given in Table 1.

Table 1. Lennard-Jones parameters (σ, ε), density (d), sidelength of the basic periodic boxe (l), number of time steps (N), and total elapsed time (t) for the five different solutions. σ and l are given in Å, ε in units of 10^{-16} erg, d in g/cm³, and t in units of 10^{-13} sec. The values for σ and ε are derived by application of Kong's [8] combination rules to data obtained by Hogervørst [9]. The numbers for N and t given in parentheses in the case of CsCl refer to the short run with the new potential.

	LiJ	LiCl	NaCl	CsCl	CsF
σ_{+-}	3.36	2.98	3.09	3.65	3.46
ε_{+-}	35.4934	28.9742	46.7208	128.935	52.8779
σ_{++}	2.37		2.73	3.92	
ε_{++}	24.7996		31.1472	185.435	
σ_{+w}	2.78		2.93	3.58	
ε_{+w}	31.048		38.878	84.2381	
σ_{--}	3.92		3.36	2.73	
ε_{--}	185.435		97.7878	31.1472	
σ_{-w}	3.58		3.24	2.93	
ε_{-w}	84.2381		70.0009	38.878	
σ_{ww}			3.10		
ε_{ww}			52.605		
d	1.19	1.05	1.08	1.25	1.27
l	18.681	18.397	18.420	18.737	18.476
N	3291	3398	3443	8000 (410)	3588
t	3.587	3.704	3.753	8.72 (0.447)	3.911

Again, 200 water molecules, 8 cations and 8 anions, equivalent to 2.2 molal solutions, have been employed. The densities, d, used in the calculations, the sidelength of the basic periodic box, l, the number of time steps, N, and the total elapsed time, t, are also given in Table 1.

Selected effective pair potentials are shown in Fig. 1 for ion-ion interactions and in Fig. 2 for ion-water interactions. Because of the strong difference in interaction energies three different cut-off parameters have been chosen: 7.11 Å for water-water, 0.5 l for ion-water and 2.5 l for ion-ion interactions.

The calculated properties of the CsCl solution, in so far as they have been obtained in the previous

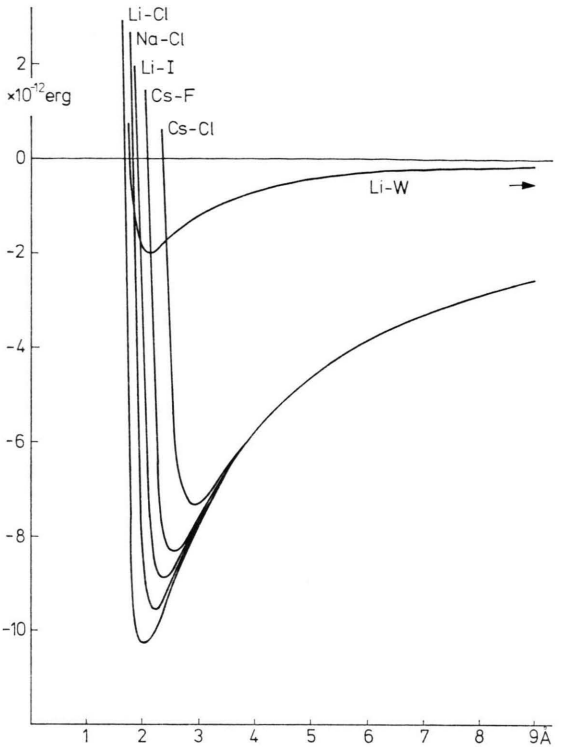

Fig. 1. Effective pair potentials for ion-ion interactions. For comparison the Li^+-water pair potential is included. The arrow marks the remaining ion-ion interaction energy at the cut-off distance 5/2 l.

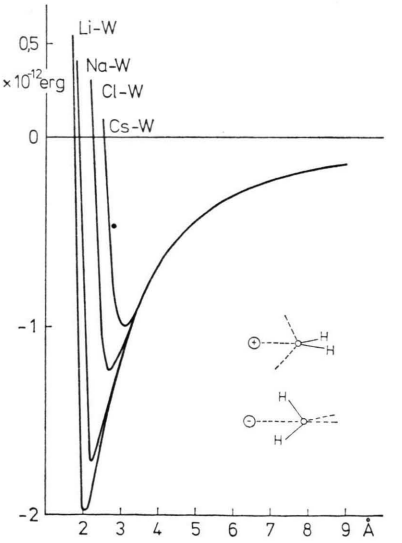

Fig. 2. Effective pair potentials for ion-water interactions. The interaction energies are given for the water molecule orientations shown in the lower right part of the figure. The point marks the minimum of the water-water interaction energy for the most favorable orientation of the two water molecules.

paper [2], are repeated here. Newly calculated properties of this solution are from a short run over 410 time steps and are therefore of limited statistical value. The difference in the ion-ion pair potentials used here and the previous paper [2] does not lead to remarkable differences in the results as far as can be judged from this short run.

For equilibration all systems were run about 1000 time steps at 900 K and another 3000 at 300 K before data were collected. Then the temperature was kept in the range 295 – 305 K. For further details of the calculations see Reference [2].

III. Results and Discussion

A) Radial Pair Correlation Functions

The radial pair correlation functions $g_{+O}(r)$, $g_{+H}(r)$, $g_{-O}(r)$, $g_{-H}(r)$ and $g_{OO}(r)$, giving the oxygen and hydrogen atom densities about the cations, anions and oxygen atoms, relative to the respective mean densities, and the corresponding total numbers of oxygen and hydrogen atoms in spheres of radius r about the ions and oxygen atoms which shall be called running integration numbers $n(r)$ are shown in Figures 3 – 5. The functions $g_{XH}(r)$ and $n_{XH}(r)$ give information about the orientation of the water molecules and shall be discussed in Section B.

Some characteristic values of the functions $g_{XO}(r)$ are given in Table 2. It can be seen from this Table that in the limits of uncertainty r_{M1} as well as R_1 does not depend on the counterion as far as the ion-water interaction is concerned. In the case of the water-water interaction r_{M1} does not depend on the solute but is shifted 0.05 Å to longer distances relative to pure water, and R_1 is smaller by 0.1 Å in the LiJ solution than in the other solutions and pure water. The R_2 values which reflect the asymmetry of the first peak, change with the counterion and, for $g_{OO}(r)$, with the solution, but no special trend is recognizable.

The r_{M1} values obtained in this work are compared in Table 3 with other available information, and are discussed in detail below. The height of the first peak, $g_{XO}(r_{M1})$, depends on the counterion, as can be seen for Li^+ and Cl^-. It increases with increasing counterion size, indicating that large counterions disturb the hydration shell less than small ones. The uncertainty in the case of Cs^+ is too large to be used as argument against this conclusion. The

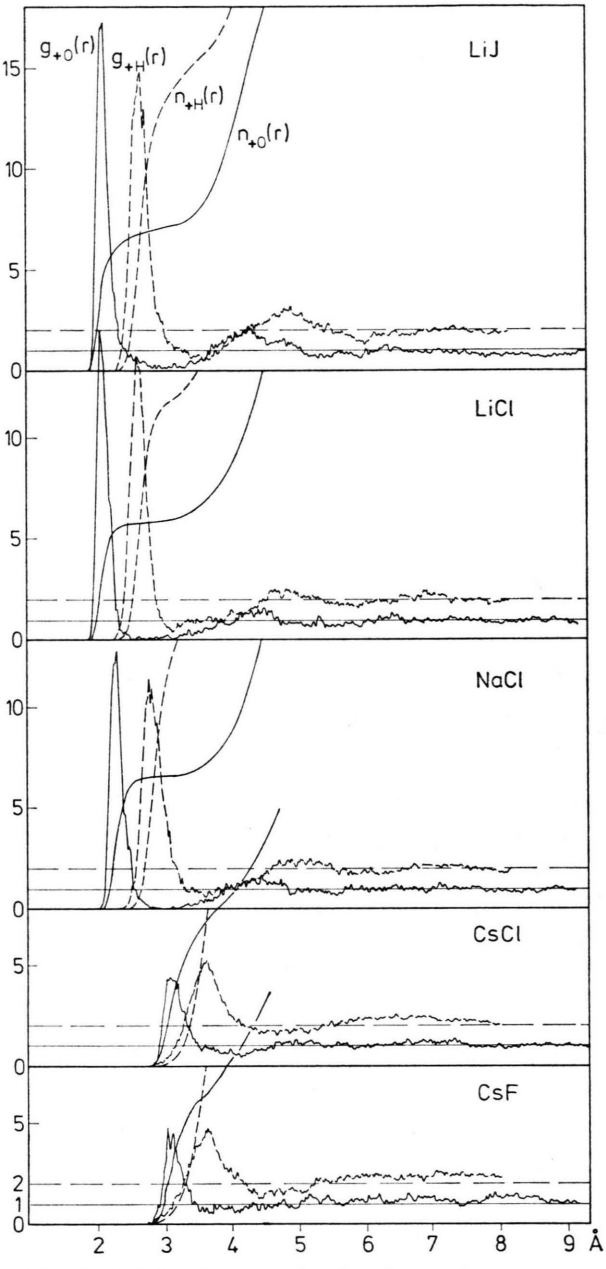

Fig. 3. Radial pair correlation functions and running integration numbers for cation-oxygen and cation-hydrogen in the five different alkali halide solutions.

height $g_{OO}(r_{M1})$ does, in the limits of uncertainty, not depend on the solute. The obvious difference, when compared with pure water, shows again the often recognized effect that solutes change the water structure in the same way as increasing temperature does. This effect is discussed in detail in our previous paper [2].

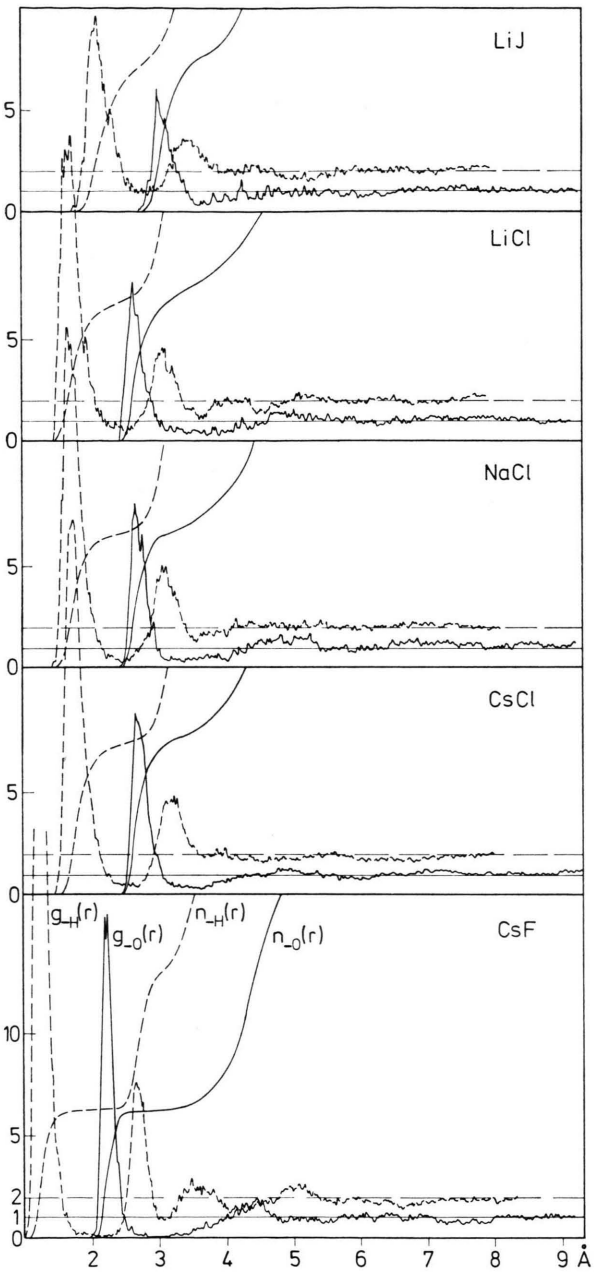

Fig. 4. Radial pair correlation functions and running integration numbers for anion-oxygen and anion-hydrogen in the five alkali halide solutions.

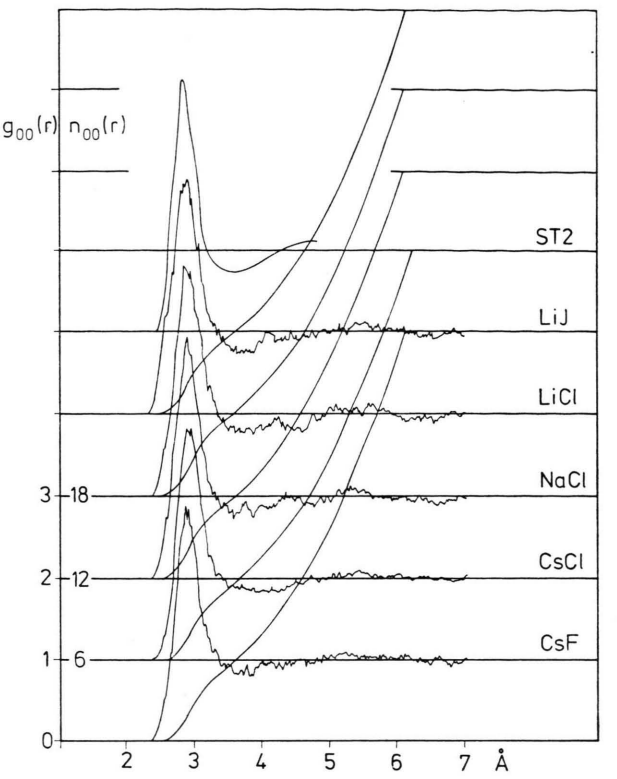

Fig. 5. Radial pair correlation function and running integration number for oxygen-oxygen in pure ST2 water [5] and the five alkali halide solutions.

The small ions Li^+ and F^- are able to form a second hydration shell in LiJ and CsF solutions as can be seen from Figs. 3 and 4 and the last four columns of Table 2, although the concentrations are as high as 2.2 molal. In the LiCl solution the second hydration shell of Li^+ is less pronounced than in LiJ because of the stronger disturbance by the smaller counterion. From the uncertainties of r_{m1}, $g_{IO}(r_{m1})$ and $g_{IO}(r_{M2})$ the general trend, also recognizable in $g_{JO}(r_{M1})$, is obvious that the hydration shell structure becomes less pronounced with increasing ion size and decreasing size of the counterion. A certain exception from this trend is shown by $g_{NaO}(r_{m1})$. An irregular behaviour of the NaCl solution will also be seen later on in the case of other properties. There are no noticeable differences in $g_{OO}(r)$ beyond statistical uncertainty between the various solutions investigated, but relative to pure water r_{M2} and r_{m1} are shifted to longer distances. At a distance slightly larger than the minimum, $g_{OO}(r)$ shows for all solutes except CsCl a small bump outside statistical noise. It seems to reflect the high concentration of water molecules on the opposite sides of the small ions Li^+, Na^+, and F^-.

A detailed comparison of the radial distribution functions of the CsCl solution with the results of an x-ray study is in preparation [10].

Table 2. Characteristic values of the radial pair correlation functions $g_{XO}(r)$ for five different alkali halide solutions. R_i, r_{Mi} and r_{mi} give the distances in Å where for the ith time $g_{XO}(r)$ is unity, has a maximum and a minimum, respectively. The values for pure water are taken from Stillinger and Rahman [5] by interpolating between 10 °C and 41 °C. The uncertainties in R_i, r_{Mi} and r_{mi} are less than ±0.02 if not stated otherwise. A general statement about the uncertainties in the g_{XO}-values is not possible; in each case it has to be estimated from the statistical noise as shown in Figures 3–5.

X	Solute	R_1[Å]	r_{M1}[Å]	$g_{XO}(r_{M1})$	R_2[Å]	r_{m1}[Å]	$g_{XO}(r_{m1})$	r_{M2}[Å]	$g_{XO}(r_{M2})$
Li^+	LiJ	1.97	2.10	17.29	2.47	3.1 ±0.2	0.12	4.30	2.24
	LiCl	1.95	2.06	15.30	2.34	2.72±0.20	0.04	4.5 ±0.1	1.6
Na^+	NaCl	2.14	2.31	12.77	2.57	3.11	0.011	4.5 ±0.1	1.6
Cs^+	CsCl	2.92	3.10±0.06	4.38	3.50	4.14	0.43	4.9 ±0.3	1.3
	CsF	2.93	3.10±0.04	≈ 4.7	3.45±0.05	3.9±0.2	0.5	5.30±0.15	1.4
F^-	CsF	2.09	2.22	≈15.8	2.49	2.92	0.03	4.46	1.88
Cl^-	LiCl	2.50	2.68	7.77	3.05±0.05	3.88±0.10	0.25	5.1 ±0.4	1.5
	NaCl	2.51	2.66	8.0	2.96	3.40±0.10	0.18	5.0 ±0.2	1.6
	CsCl	2.51	2.66	8.93	3.04	3.55±0.10	0.27	4.85±0.10	1.28
J^-	LiJ	2.88	3.02	≦6.0	3.47±0.04	3.7 ±0.1	0.30	4.8 ±0.5	1.4
O	LiJ	2.54	2.90	2.87	3.37±0.05	3.75±0.15	0.75	5.45±0.10	1.13
	LiCl	2.63	2.90±0.04	2.81	3.33	3.75±0.15	0.77	5.3 ±0.3	1.15
	NaCl	2.63	2.90	2.96	3.30±0.04	3.73±0.15	0.74	5.30±0.10	1.13
	CsCl	2.66	2.91±0.04	2.82	3.40	4.08±0.15	0.82	5.40	1.09
	CsF	2.63	2.90	2.87	3.35	3.82	0.78	5.20±0.10	1.07
	pure water	2.63	2.85	3.13	3.19	3.53	0.72	4.70	1.13

The position of the first peak of the $g_{XO}(r)$ functions (see Table 2) giving the average ion-oxygen distance of the first hydration shell and the nearest neighbour oxygen-oxygen distance are compared in Table 3 with the results of x-ray diffraction studies [11–14], crystal radii data [15] and preliminary results of Monte Carlo calculations [16]. There is excellent agreement between the different methods for the nearest neighbour oxygen-oxygen distance. In the case of the cations the agreement between molecular dynamics, x-ray diffraction and Monte Carlo calculations is good, while the sum of the crystal radii of ion and water lead to values which are remarkably higher. There are large discrepancies between the different methods in the case of the anions. Obviously the molecular dynamics values are remarkably lower when compared with the other ones. In particular the good agreement between the various x-ray measurements for Cl^- raises some doubt about the molecular dynamics results. Agreement in the case of cations and disagreement in the case of anions might indicate that the asymmetric charge distribution in the ST2 water model causes this discrepancy. The ST2 model leading to satisfactory results for pure water might not be fully appropriate to describe aqueous solutions.

Table 3. Average ion-oxygen distances of the first hydration shell and nearest neighbour oxygen-oxygen distances deduced from molecular dynamics calculations, x-ray-investigations, crystal radii data and preliminary Monte Carlo calculations. a) Ref. [11], b) Ref. [12], c) Ref. [13], d) Ref. [14].

	molecular dynamics	x-ray	crystal radii [15]	Monte Carlo [16]
Li^+	2.08	1.95 [a], 2.1 [b]	2.35	1.95
Na^+	2.31	—	2.66	2.35
Cs^+	3.10	3.14 [c]	3.25	—
F^-	2.22	—	2.64	2.75
Cl^-	2.67	3.10 [a], 3.15 [d], 2.9–3.25 [b]	3.10	3.45
J^-	3.02	3.69 [d]	3.46	—
H_2O	2.90	2.85 [a], 2.90 [b], 2.92 [d]	2.90 [b, d]	2.90

The hydration numbers for the various ions are defined in this paper as the numbers of oxygen atoms within a sphere of radius r_{m1}. They are given in Table 4. The ranges merely reflect the uncertainties in positioning the minima. For the small ions

Table 4. Hydration numbers deduced from the radial pair correlation functions. The upper right and lower left numbers are anion and cation hydration numbers respectively. The ranges merely indicate the statistical uncertainty in r_{m1}.

	F	Cl	I
Li		7.4±0.4	7.3±0.3
	5.7±0.2	7.1±0.1	
Na		6.7±0.3	
	6.6±0.1		
Cs	6.3±0.1	7.9±0.3	
	7.3±0.7	8.2±0.8	

Li^+, F^- and Na^+ where the end of the first hydration shell is clearly given by the pronounced minimum in $g_{XO}(r)$, the hydration numbers are well defined and easily recognized by the plateau in $n_{XO}(r)$. With increasing ion size, where the hydration shell becomes less pronounced, the determination of the hydration numbers is less certain as there is no plateau in $n_{XO}(r)$.

Our hydration numbers increase with ion size as expected from steric reasons, with the one exception of the couple Cl^- and J^- with Li^+ as counterion where they are the same. At lower concentration and/or with larger counterions this exception might not exist. The hydration numbers also increase with increasing size of the counterion [17]. This results from the fact that large counterions disturb the hydration shell less than small ones, an effect which is also recognizable in the formation of the second hydration shell as noted above. Again the NaCl solution is an exception. The hydration number of Cl^- in this solution is smaller than in the LiCl solution. It should be pointed out that the dependence of the hydration number on the size of the counterion leads to a larger hydration number for Li^+ in LiJ than for Na^+ in NaCl.

The molecular dynamics calculations so far do not give any hint for distinguishing between coordination and solvation numbers on the basis of non-oriented water molecules in the hydration shells of the ions, as discussed e. g. by Bockris and Saluja [18]. A detailed comparison of hydration numbers derived from molecular dynamics calculations with those deduced from other investigations will be given in a separate paper.

The number of nearest neighbours of a water molecule as deduced from the integration of $g_{OO}(r)$ up to the minimum is noticeable larger for the solutions than for pure ST2 water. Quantitative differences between the various solutions cannot be given because of the statistical uncertainty, as can be seen from Figure 5. But if the integration is extended to a fixed distance, r', e. g. the minimum of the $g_{OO}(r)$-curve of pure water, then $n(r')$ is the same for all solutions, namely six, and about 10% higher than for pure water. From this fact it can be seen again that the water in aqueous solutions shows features of pure water at elevated temperature as well as of water under compression.

The interionic radial pair correlation functions $g_{+-}(r)$ show no ion pairing except in the case of

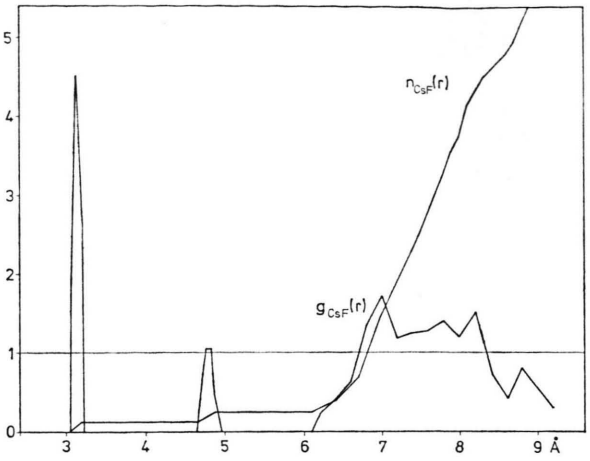

Fig. 6. Radial ionic pair correlation function and running integration number for cesium-fluorine.

cesiumfluoride which is shown in Figure 6 [19]. Inspite of the poor statistics, caused by the small number of ions, the very sharp peak at 3.14 Å shows, in agreement with the x-ray diffraction studies of Bertagnolli, Weidner and Zimmermann [13] that fluorine ions occupy places of water molecules in the first hydration shell of Cs^+. From the running integration number $n_{CsF}(r)$ it can be infered that about one out of ten F^- are placed in the first hydration shell of Cs^+ in the case of a 2.2 molal solution as investigated here.

B) Orientation of the Water Molecules

The orientation of the water molecules around the ions can be seen from the radial pair correlation functions $g_{+H}(r)$ and $g_{-H}(r)$ (Figs. 3 and 4), and from the average value of $\cos\Theta$ as a function of r (Figs. 7 and 8), Θ being the angle between the dipole moment of a water molecule and the vector pointing from the oxygen atom towards an ion.

As can be seen from Fig. 4 for all five solutions investigated, the distances between the first peaks of $g_{-H}(r)$ and $g_{-O}(r)$ are 1 Å, the O – H distance in the rigid ST2 water model, and the integration numbers $n_{-H}(R_2)$ and $n_{-O}(R_2)$ are equal. Therefore, it has been concluded that in the case of the anions a linear hydrogen bond is being formed. This orientation of the water molecules around the anions has been found for Cl^- by x-ray and neutron diffraction studies [11] and for F^- by NMR measurements [20]. In the case of the cations the positions of

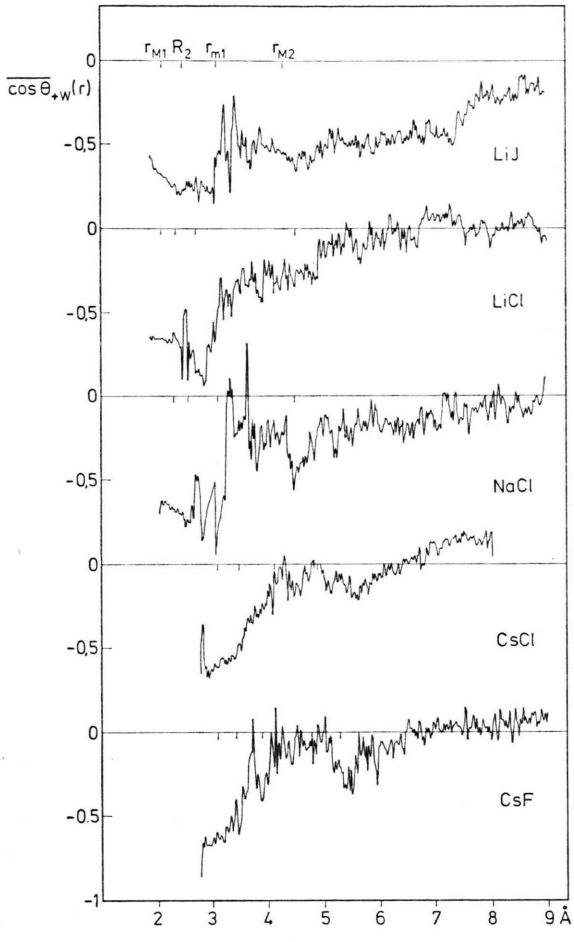

Fig. 7. Average value of $\cos\Theta_{+W}$ as a function of distance between cation and oxygen for five different alkali halide solutions. Θ_{+W} is the angle between the two vectors connecting the oxygen atom with the cation and with the center of mass of the water molecule. The positions of r_{M1}, R_2, r_{m1} and r_{M2} are taken from Table 2.

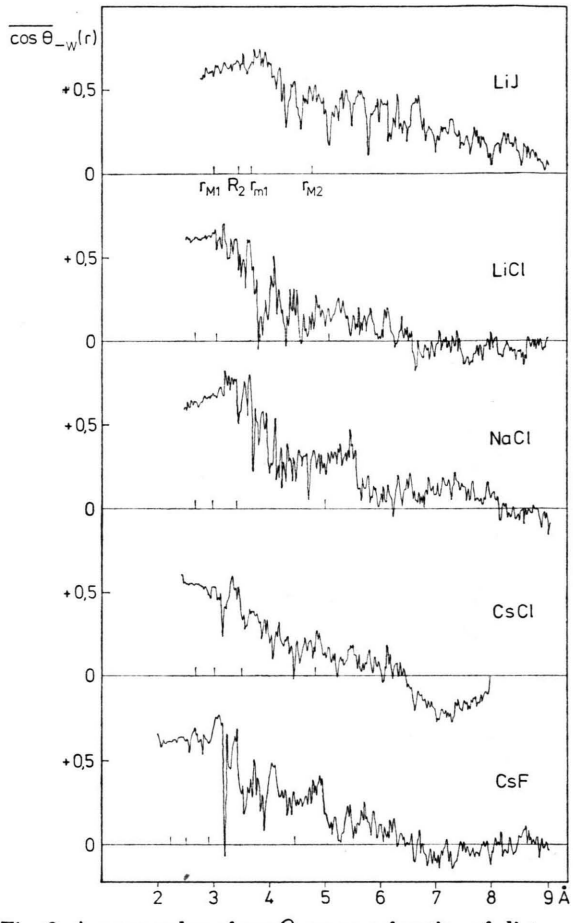

Fig. 8. Average value of $\cos\Theta_{-W}$ as a function of distance between anion and oxygen for five different alkali halide solutions. Θ_{-W} is the angle between the two vectors connecting the oxygen atom with the anion and with the center of mass of the water molecule. The positions of r_{M1}, R_2, r_{m1} and r_{M2} are taken from Table 2.

the first peaks of the $g_{+H}(r)$ curves obey the relation

$$r_{M1}^{+H} = [(r_{M1}^{+O})^2 + \tfrac{2}{3} r_{M1}^{+O} R_{OH} + (R_{OH})^2]^{1/2},$$

where $R_{OH} = 1$ Å and r_{M1}^{+O} is the position of the first peak of a $g_{+O}(r)$ curve. This allows the conclusion that a lone pair orbital of the water molecules is directed towards the cation. It agrees with these conclusions that the values of $\langle\cos\Theta(r)\rangle$, given in Figs. 7 and 8, are about -0.6 and $+0.6$, for cations and anions respectively, in the ranges $0 \leqq r \leqq R_2$.

The distribution functions $P(\cos\Theta)$ in the first hydration shells of Cs^+ and F^- in the CsF solution and the respective mean values $\langle\cos\Theta\rangle$ are shown in Figure 9. A measure of the width of such curves is the average square deviation from the mean value. The $\langle\cos\Theta\rangle$-values and the average square deviations for the five solutions studied in this paper are collected in Table 5.

As all water molecules in the first hydration shell ($0 \leqq r \leqq r_{m1}$) are included, not only the water molecules in the range $0 \leqq r \leqq R_2$ where $\langle\cos\Theta(r)\rangle$ is rather constant at -0.6 and $+0.6$ for cations and anions respectively, a positive tail arises in the $P_{CsW}(\cos\Theta)$-curves. This is a consequence of strongly decreasing orientation of the water molecules with increasing distance in the case of the large cations. As can be seen from Table 5, the

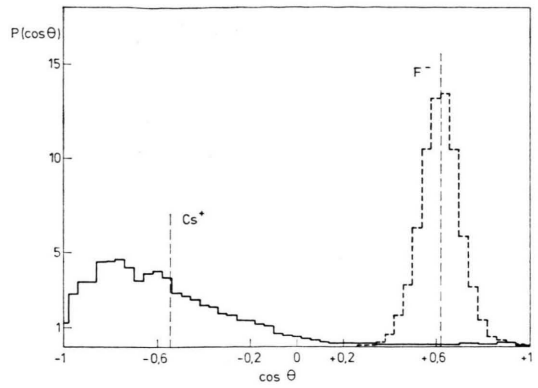

Fig. 9. Distribution function of $\cos\Theta$ for the water molecules in the first hydration shells of the ions in a CsF solution. $P(\cos\Theta)$ is given in arbitrary units. The dashed lines indicate the mean value of $\cos\Theta$.

Table 5. Mean values of $\cos\Theta$ and in parenthesis average square deviations from the mean values for the water molecules in the hydration shells of the ions in five different alkali halide solutions. The upper right and lower left numbers refer to anions and cations respectively.

	F	Cl	J
Li	—	+0.58 (0.057)	+0.63 (0.033)
		−0.66 (0.012)	−0.69 (0.016)
Na	—	+0.65 (0.020)	—
		−0.69 (0.019)	
Cs	+0.62 (0.009)	+0.52 (0.039)	—
	−0.55 (0.128)	−0.55 (0.138)	

sharpness of the distribution functions $P(\cos\Theta)$ decreases with increasing cation size, but a similar trend is not recognizable for the anions. There is no clear trend in respect to the size of the counterions.

Some general features of $\langle\cos\Theta(r)\rangle$ are recognizable for all ion-water interactions (Figs. 7 and 8). The plateau-like range at small distances is followed by an area of strong statistical noise, a consequence of the small number of water molecules in the region of the minimum of the radial pair correlation functions $g_{IO}(r)$. The $\langle\cos\Theta(r)\rangle$ falls off to zero more or less rapidly, indicating the different range of orienting power of the different ions.

A few remarkable differences between the various solutes should be mentioned. The fluctuations of $\langle\cos\Theta(r)\rangle$ in the ranges $0 \leqq r \leqq R_2$ are smaller for the anions $(+0.60 \pm 0.07)$ than for the cations (-0.65 ± 0.15), indicating a stronger orientation of the water molecules in these ranges around the anions. The large Cs^+ shows no real plateau, there is a steady increase of $\langle\cos\Theta_{CsW}(r)\rangle$ throughout the first hydration shell. The peaks at small distances, where the radial pair distribution function is almost zero, appear to be single events caused by the unfavorable orientation of a water molecule between a Cs^+ and the counterion, especially pronounced in this case because of the small orienting power of Cs^+. The differences in statistical noise in the area of r_{m1} for the various solutes are directly related to the values of $g_{IO}(r_{m1})$ and the number of time steps calculated. The formation of a second hydration shell is also reflected in $\langle\cos\Theta(r)\rangle$. In the respective regions Li^+, F^-, and Cl^- in NaCl show a kind of plateau indicating a preferential orientation at these distances. The LiJ solution is strongly different from all the others in respect to the falling off of $\langle\cos\Theta(r)\rangle$ with increasing distance. Over the whole range 3.5 – 7.5 Å $\langle\cos\Theta_{LiW}(r)\rangle$ is nearly constant at about -0.5, while $\langle\cos\Theta_{JW}(r)\rangle$ is indeed decreasing steadily but much slower when compared with the other solutions. This strongly different behaviour results from the orienting power of the small Li^+ combined with the fact that the large counterion J^- disturbs the hydration shell of Li^+ only slightly. The orientation around Li^+ is of course reflected in $\langle\cos\Theta_{JW}(r)\rangle$ too.

The average value of the cosine of the angle between the dipole moments of two water molecules is given as a function of distance between the oxygen atoms of the two water molecules in Fig. 10 for the five different alkali halide solutions. The plots for all of the solutions except LiJ are very similar. At small distances an angle between the dipole moments of about half of a tetrahedral angle is preferred. Over the range of the first peak in the radial distribution functions $g_{OO}(r)$, $\langle\cos\Theta_{WW}(r)\rangle$ falls off rapidly to zero indicating no preferential orientation in the region of the minimum of $g_{OO}(r)$. For larger r, $\langle\cos\Theta_{WW}(r)\rangle$ becomes negative showing that for distances of more than 4 Å the angular distribution is not isotropic but there exists a slight preference for angles larger than 90°. The LiJ solution shows an r dependence of $\langle\cos\Theta_{WW}(r)\rangle$ remarkably different from the other solutions. Starting at smaller values $\langle\cos\Theta_{WW}(r)\rangle$ reaches with 0.56 a maximum in the range of the first peak of $g_{OO}(r)$ corresponding again to half of the tetra-

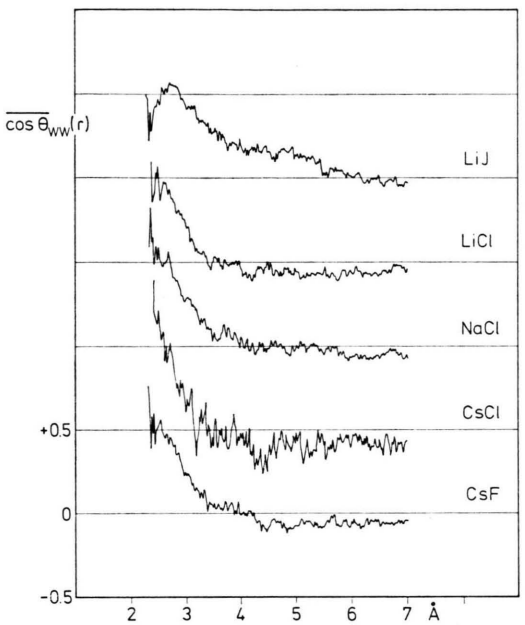

Fig. 10. Average value of $\cos\Theta_{WW}$ as a function of distance between the oxygen atoms of two water molecules for five different alkali halide solutions. Θ_{WW} is the angle between the dipol moment vectors of the two water molecules. The stronger statistical noise in the case of CsCl results from the fact that $\langle\cos\Theta_{WW}\rangle$ data have been collected only over about 500 time steps.

hedral angle. From the maximum on it decreases slowly to zero indicating an isotropic angular distribution not before 6 Å. This slow decrease reflects the long range orientation of the water molecules around Li^+ and J^- as can be seen from $\langle\cos\Theta_{LiW}(r)\rangle$ and $\langle\cos\Theta_{JW}(r)\rangle$ in Figs. 7 and 8. The orientation around the ions prevents an isotropic angular distribution of the water molecules around each other.

Denoting the unit vector in the dipole moment direction of water molecule i by $\boldsymbol{m}_i$ then $\boldsymbol{M}$ is defined by

$$\boldsymbol{M} = \sum_i \boldsymbol{m}_i .$$

The quantity $\langle M^2\rangle/N$, where N is the total number of water molecules in the basic periodic box, has been calculated for the five different alkali halide solutions and is given in Table 6 together with the value for pure ST2 water as calculated by Stillinger and Rahman [5]. For all five 2.2 molal solutions the values are larger than for pure water but smaller than one, indicating less correlation between the dipole moment vector directions. It can be seen from Table 6 that the deviation from pure water is

Table 6. $\langle M^2\rangle/N$ for five different alkali halide solutions and pure ST2 water. a) This value is an average over only about 500 time steps and therefore uncertain. b) Ref. [5].

Solute	LiJ	LiCl	NaCl	CsCl	CsF	pure ST2-water
$\langle M^2\rangle/N$	0.44	0.34	0.32	(0.39) [a]	0.17	0.15 [b]

smallest in the case of CsF and increases with increasing anion size. There is practically no cation dependence for the three different chloride solutions. This order of $\langle M^2\rangle/N$ is in agreement with the structure breaking ability of the anions as deduced from various other kinds of measurements (see e. g. Verrall [21]).

It appears to be premature to try to relate at this stage the quantities $\langle\cos\Theta_{WW}(r)\rangle$ and $\langle M^2\rangle/N$ calculated here to measured static dielectric properties of aqueous solutions.

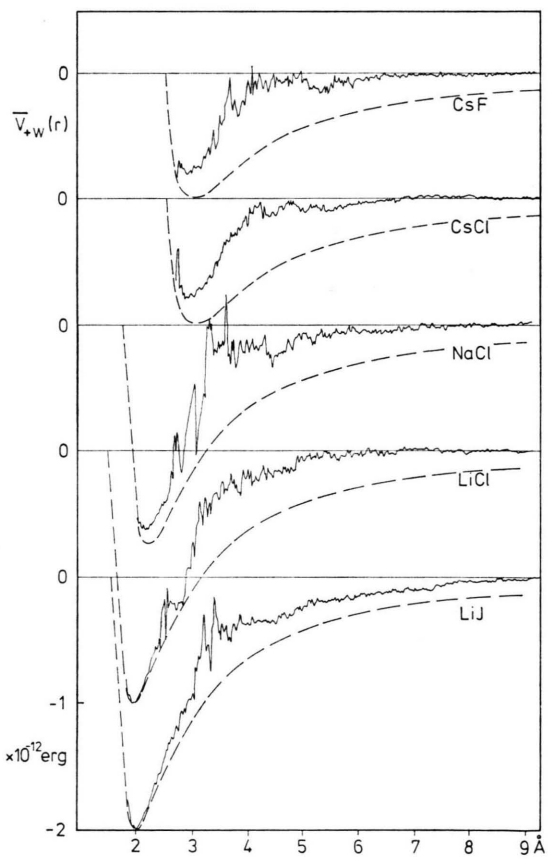

Fig. 11. Average potential energy of a water molecule in the field of cations as a function of ion-oxygen distance for five different alkali halide solutions. The broken lines show the effective pair potential for $\cos\Theta_{+W} = -1$.

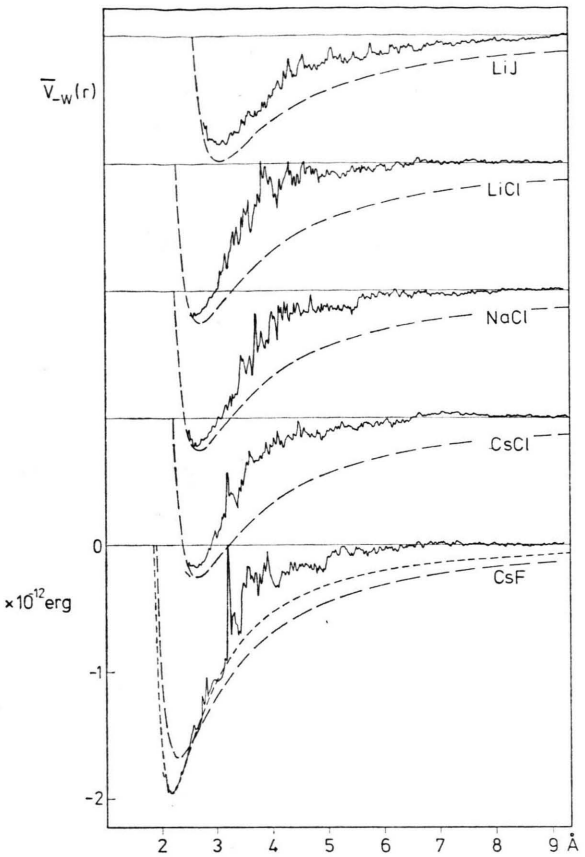

Fig. 12. Average potential energy of a water molecule in the field of anions as a function of ion-oxygen distance for five different alkali halide solutions. The broken lines show the effective pair potential for $\cos\Theta_{-W}=1$; the dashed line in the case of CsF corresponds to the linear hydrogen bond configuration $F^- \ldots H-O\diagdown_{H}$.

C) Average Potential Energy

In Figs. 11 and 12 the average potential energies of a water molecule in the field of a cation or anion, respectively, are shown as functions of the ion-oxygen distance. In addition the effective pair potentials between the various ions and a water molecule are given as broken lines for the case in which $\cos\Theta_{+W} = -1$ and $\cos\Theta_{-W}=1$. These configurations yield the lowest minimum in the effective pair potential for all ions except F^-. In the case of the fluorine ion the lowest pair interaction energy minimum is realised by the formation of a linear hydrogen bond $F^- \ldots H-O\diagdown_{H}$. The pair potential for this configuration is given as a dashed line in Figure 12. For Li^+ and Cl^- the minimum energies for the two orientations differ very little. This correlation between minimum energy and orientation in the case of the rigid ST2 water molecule in the field of an ion agrees qualitatively with results of molecular orbital calculations [22]. From this agreement it can be expected that the ST2 water model leads to reasonable results also for aqueous solutions. The comparison between full and broken lines for the various ions in the five different alkali halide solutions shows the strong orienting influence of neighbouring water molecules and ions, leading to a more or less unfavorable orientation in respect to the central ion. As the potential energy of a water molecule in the field of an ion depends, besides on r, on the orientation of the water molecule, many similarities arise in the curves of $\langle \cos\Theta_{IW}(r)\rangle$ and $\langle V_{IW}(r)\rangle$ (cf. Figs. 7, 8, 11, 12).

In Fig. 13 the average water-water pair potential energy is given as a function of oxygen-oxygen distance for the five alkali halide solutions. In all five solutions water molecules at small distances with positive pair interaction energies have been found.

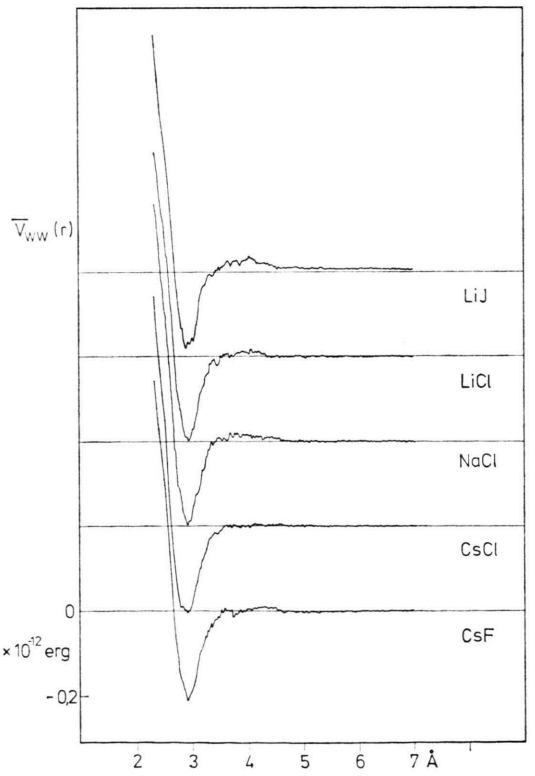

Fig. 13. Average pair potential energy of the water molecules as a function of oxygen-oxygen distance for five different alkali halide solutions.

The minimum of $\langle V_{WW}(r) \rangle$ coincides with the maximum of the first peak in the radial pair correlation function $g_{OO}(r)$ and ranges from -2.6 for LiJ to -3.1 kcal/mole for CsF. Between 3.5 and 4.5 Å the average potential energy is either zero (in the case of CsCl) or positive. Beyond 4.5 Å it is zero except for LiJ, where $\langle V_{WW}(r) \rangle$ remains positive up to the cut-off distance. The positive values of $\langle V_{WW}(r) \rangle$ in the range $3.5-4.5$ Å result from the orientation of the water molecules around the ions leading to unfavorable orientations of the water molecules relative to each other. A comparison of $\langle V_{WW}(r) \rangle$ with $\langle \cos \Theta_{LiW}(r) \rangle$ and $\langle \cos \Theta_{JW}(r) \rangle$ in the case of the LiJ solution shows this effect very clearly.

D) Pair Interaction Energy Distribution

Denoting the average number of pairs having an interaction energy in the range of dV by $p(V)dV$, the cation-water, anion-water and water-water pair interaction energy distribution functions $p(V)$ are

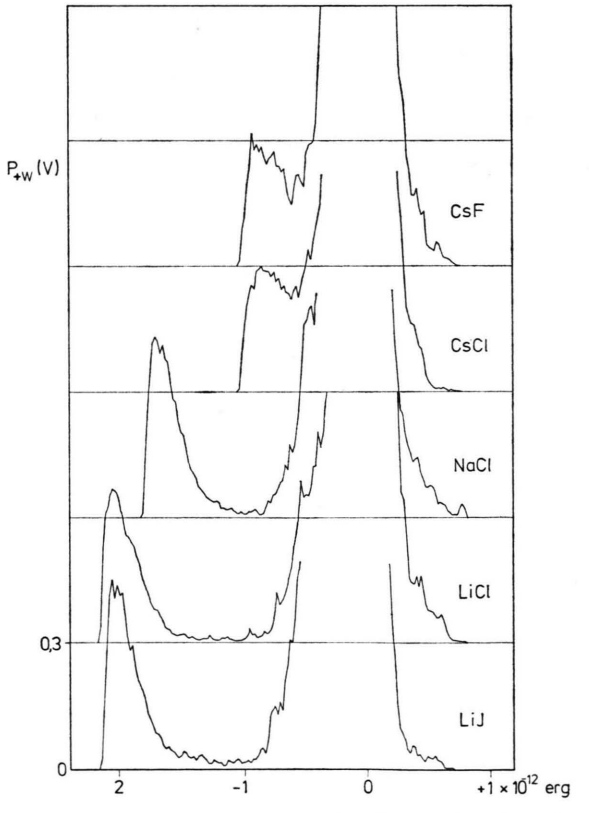

Fig. 14. Pair interaction energy distribution functions for cations-water in five different alkali halide solutions. $p(V)$ is given in arbitrary units.

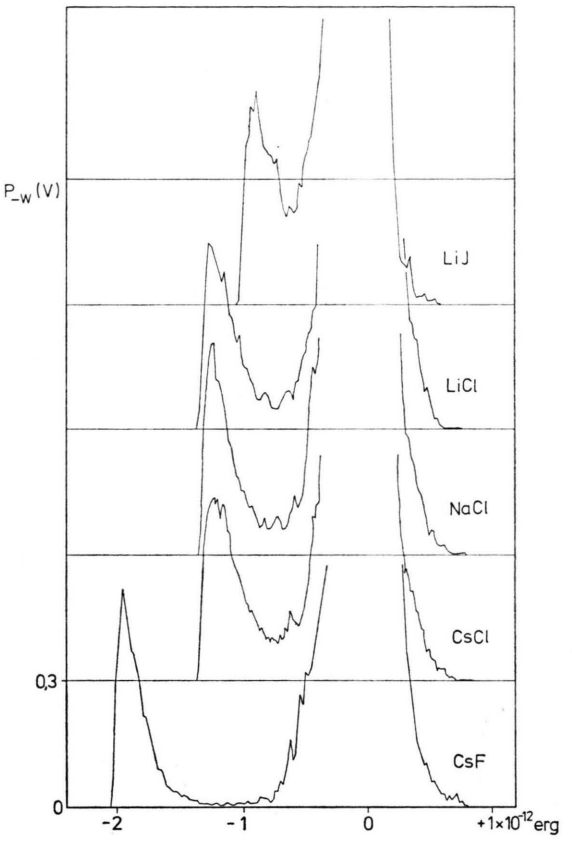

Fig. 15. Pair interaction energy distribution functions for anions-water in five different alkali halide solutions. $p(V)$ is given in arbitrary units.

shown in Figs. $14-16$ respectively. $p(V)$ is given in arbitrary units. It increases rapidly as V goes to zero because of the greater number of pair interactions at large distances where coulombic terms of the potential are small.

The negative energy sides of the plots in Figs. 14 and 15 reflect the more or less pronounced hydration shells of the ions as expected from the radial distribution functions together with the average potential energy plots. Comparing ions of similar size like Cs^+ and J^-, it can be seen that the anions show a less uniform energy distribution than the cations. There are no distinct differences recognizable in the $p(V)$ plots for different counterions as can be seen for Cl^- in Figure 15. The positive tails end between 7 and $8 \cdot 10^{-13}$ erg for all ions in the various solutions except J^- where it ends at about $6 \cdot 10^{-13}$ erg. The positive values of the pair potential arise from unfavorable water molecule orienta-

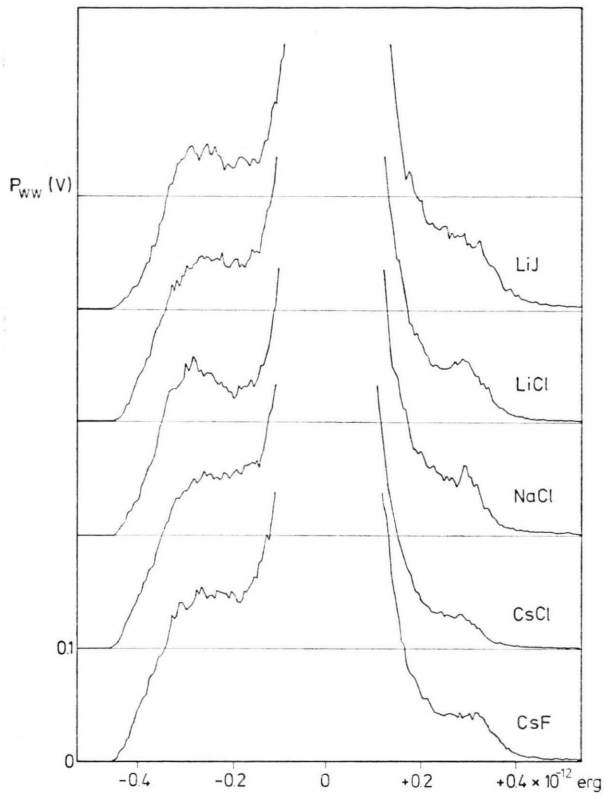

Fig. 16. Pair interaction energy distribution functions for water-water in five different alkali halide solutions. $p(V)$ is given in arbitrary units.

tions due to the hydration shells of counterions and from water molecules located in positions intermediate between hydration shells. It should be noted that the number of water molecules with positive energies is obviously smallest in the LJ solution, recognizable in the J^--water as well as in the Li^+-water pair interaction energy distribution. This results from the long range ordering of the water molecules in this solution as can be seen from the $\langle \cos \Theta(r) \rangle$ and correspondingly the $\langle V(r) \rangle$ plots for both ions Li^+ and J^-.

In Fig. 16 the water-water energy distribution in the five alkali halide solutions are shown. As discussed in detail in a previos paper [2], the plateau at negative energies demonstrates that these solutions show properties of pure water at elevated temperatures while the positive energies indicate by the shoulder at about $2.8 \cdot 10^{-13}$ erg (ca. 4 kcal/mole) that the water-water interactions in these solutions show additionally features of pure water under high compression [23]. The differences between the various solutions as far as the negative energy sides are concerned are not considered to be significant at this stage of the investigations. It is obvious from the plots that the number of water-water interactions with positive energies is smallest in the case of the CsCl solution and by far the largest for the LiJ solution. This relatively high percentage of water-water interactions with positive energies in the LiJ solution results from the fact that favorable orientation of the water molecules around Li^+ and J^- leads to unfavorable orientations of the water molecules relative to each other.

E) Self Diffusion Coefficient for Water

The self diffusion coefficients for the water molecules calculated here using the relationship

$$D = \lim_{t \to \infty} \left\langle \frac{[R(t) - R(0)]^2}{6t} \right\rangle$$

are for all five solutions by more than a factor of two larger than the ones obtained by Endom, Hertz, Thül, and Zeidler [24] from NMR measurements. The reason for this discrepancy is most probably that the simulation time was not long enough to reach the limiting slope.

Acknowledgements

Stimulating discussions with Prof. Dr. A. Klemm, Dr. L. Schäfer and Dipl. Phys. P. Bopp are gratefully acknowledged.

[1] K. Heinzinger and P. C. Vogel, Z. Naturforsch. **29 a**, 1164 [1974].
[2] P. C. Vogel and K. Heinzinger, Z. Naturforsch. **30 a**, 789 [1975].
[3] E. M. Gosling and K. Singer, Cecam Report of Workshop on Ionic Liquids, 1974, p. 242.
[4] A. Rahman, Cecam Report of Workshop on Ionic Liquids, 1974, p. 263.
[5] F. H. Stillinger and A. Rahman, J. Chem. Phys. **60**, 1545 [1974].
[6] P. C. Vogel and K. Heinzinger, Z. Naturforsch. **31 a**, 476 [1976].
[7] A. Rahman and F. H. Stillinger, J. Chem. Phys. **55**, 3336 [1971].
[8] C. L. Kong, J. Chem. Phys. **59**, 2464 [1973].
[9] W. Hogervørst, Physica **51**, 59, 77 [1971].
[10] G. Pálinkás, private communication.
[11] A. H. Narten, F. Vaslow, and H. A. Levy, J. Chem. Phys. **58**, 5017 [1973].

[12] G. Licheri, G. Piccaluga, and G. Pinna, J. Appl. Cryst. **6**, 392 [1973].

[13] H. Bertagnolli, J. U. Weidner, and H. W. Zimmermann, Ber. Bunsenges. **78**, 2 [1974].

[14] R. M. Lawrence and R. F. Kruh, J. Chem. Phys. **47**, 4758 [1967].

[15] M. P. Tosi and F. G. Fumi, J. Phys. Chem. Solids **25**, 45 [1964].

[16] H. Kistenmaker, H. Popkie, and E. Clementi, J. Chem. Phys. **61**, 799 [1974].

[17] G. J. Safford, P. S. Leung, and S. M. Sanborn, Research and Development Progress Report No. 590, U.S. Dept. of the Interior, 1970.

[18] J. O'M. Bockris and P. P. S. Saluja, J. Phys. Chem. **76**, 2298 [1972].

[19] There seems to be general agreement in the literature that no ion pairing occurs in LiCl and NaCl solutions at these concentrations (see e.g. R. W. Creekmore and C. N. Reilley, J. Phys. Chem. **73**, 1563 [1969]), but that it might occur in cesium-halide solutions with increasing tendency for decreasing halide ion size (see e.g. Ref. [14]).

[20] H. G. Hertz and C. Rädle, Ber. Bunsenges. **77**, 521 [1973].

[21] R. E. Verrall, in: Water, a Comprehensive Treatise, F. Franks (ed.), Plenum Press, New York and London 1974, Vol. III, p. 211.

[22] P. Schuster, in: Structure of Water and Aqueous Solutions, W. A. P. Luck (ed.), Verlag Chemie, Weinheim 1974, p. 160.

[23] F. H. Stillinger and A. Rahman, J. Chem. Phys. **61**, 4973 [1974].

[24] L. Endom, H. G. Hertz, B. Thül, and M. D. Zeidler, Ber. Bunsenges. **71**, 1008 [1967].